Stark Spectroscopy of Donor/Acceptor Substituted Polyenes

Gerold U. Bublitz,[†] Rafael Ortiz,[‡] Seth R. Marder,[‡,§] and Steven G. Boxer*[,†]

Contribution from the Department of Chemistry, Stanford University, Stanford, California 94305-5080, The Beckman Institute, California Institute of Technology, Pasadena, California 91125, and the Jet Propulsion Laboratory, California Institute of Technology, Pasadena, California 91109

Received November 25, 1996[⊗]

Abstract: The electronic structure of donor/acceptor polyenes (merocyanines) is studied by means of electroabsorption (Stark) spectroscopy. Molecules belonging to this class exhibit an extreme variability of their linear and nonlinear optical properties. Depending on the nature of the donor and acceptor end groups and the polarity of their solvent environment they can adopt ground state molecular structures between limits with mostly localized double bonds (polyene-like) or fully delocalized double bonds (cyanine-like). By comparing the results obtained for the change in dipole moment, $\Delta\mu$, and change in polarizability, $\Delta\alpha$, upon optical excitation of 12 donor/acceptor polyenes with theoretical predictions, each molecule's location in between these limits can be assigned. The results demonstrate that this position can be understood by considering only the relative electron donating and accepting strengths of the end groups. The solvent dependence of the electronic structure is also studied by measuring Stark spectra for two compounds in different frozen solvents. The results are consistent with a change of the molecule's ground state toward more dipolar structures in polar solvents. Taken together, the donor, acceptor, and solvent dependences of the electronic structure of donor/acceptor polyenes can be described by a simple model based on the gradual change of the molecule's ground state between polyene-like and cyanine-like structures.

Donor/acceptor substituted polyenes or merocyanine dyes are of widespread interest. Their intense absorption bands in the visible region of the spectrum and the remarkable sensitivity of these bands to solvent polarity have been studied for a great number of dyes.[1−3] Recently the nonlinear optical coefficients of these molecules have been linked to the influence of the donor and acceptor group on the connecting polyene bridge, providing deeper insight into structure−function relationships in nonlinear optical materials.[4−7] In addition to the prospect of practical applications, these molecules also provide an ideal case for testing and furthering our theoretical understanding of the electronic structure of conjugated systems.

The effects of the electron donating and accepting end groups on the electronic structure of the bridging polyene can be modeled by the simple picture shown below.

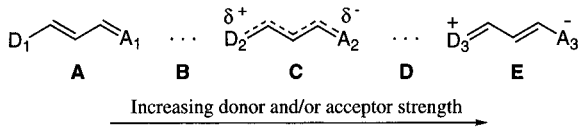

If both the donor and acceptor are weak, the molecular structure will be effectively like an unperturbed polyene (**A**). With increasing donor and/or acceptor strength the ground state structure of the bridge becomes both more delocalized and dipolar, that is it changes toward a cyanine-like fully delocalized structure (**C**). Further increase of the donor and/or acceptor strength leads to changes toward the limit of a charge-separated structure (**E**) where the double bonds are again localized, but their position has shifted relative to form **A**. There should exist a full range of intermediate cases between these limits, for example **B** would have a structure with contributions from **A** and **C**, while **D** would be an intermediate between structures **C** and **E**. Two closely related concepts to quantitate these effects are the average bond length alternation (BLA) and the average bond order alternation (BOA) between adjacent bonds in the bridge. Limit **A** corresponds to a BLA of about 0.11 Å (BOA $= -0.6$), the value found for a polyene like octatetraene, BLA $= 0$ Å (BOA $= 0$) at the cyanine limit **C**, and the BLA is negative from **C** toward the limit **E** (the BOA is positive now).[8,9]

Another way to view the effects of the donor and acceptor groups, which ties in with the experimental results presented in this paper, is that they create a substantial *internal* electric field applied along the long molecular axis. The further effect of solvent polarity on the molecular structure can be viewed as the effect of a *matrix* electric field.[10] Depending on the polarity of the solvent, the ground state structure of the solvated molecule is more (for polar solvents) or less (for nonpolar solvents) dipolar in character. This effect has been demonstrated by both IR and NMR measurements of merocyanines in different solvents,[11] each demonstrating a change in the molecular structure with

[†] Department of Chemistry, Stanford University.
[‡] The Beckman Institute, California Institute of Technology.
[§] The Jet Propulsion Laboratory, California Institute of Technology.
[⊗] Abstract published in *Advance ACS Abstracts,* March 15, 1997.

(1) Brooker, L. G. S.; Keyes, G. H.; Williams, W. W. *J. Am. Chem. Soc.* **1942**, *64*, 199−210.
(2) Brooker, L. G. S.; Keyes, G. H.; Sprague, R. H.; VanDyke, R. H.; VanLarge, E.; VanZandt, G.; White, F. L. *J. Am. Chem. Soc.* **1951**, *73*, 5326−5332.
(3) Brooker, L. G. S.; Keyes, G. H.; Sprague, R. H.; VanDyke, R. H.; VanLarge, E.; VanZandt, G.; White, F. L.; Cressman, H. W. J.; Dent, S. G. J. *J. Am. Chem. Soc.* **1951**, *73*, 5332−5350.
(4) Marder, S. R.; Perry, J. W.; Bourhill, G.; Gorman, C. B.; Tiemann, B. G.; Mansour, K. *Science* **1993**, *261*, 186−189.
(5) Gorman, C. B.; Marder, S. R. *Proc. Natl. Acad. Sci. U.S.A.* **1993**, *90*, 11297−11301.
(6) Marder, S. R.; Cheng, L.-T.; Tiemann, B. G.; Friedli, A. C.; Blanchard-Desce, M.; Perry, J. W.; Skindhøj, J. *Science* **1994**, *263*, 511−514.
(7) Marder, S. R.; Gorman, C. B.; Meyers, F.; Perry, J. W.; Bourhill, G.; Brédas, J.-L.; Pierce, B. M. *Science* **1994**, *265*, 632−635.
(8) Marder, S. R.; Perry, J. W.; Tiemann, B. G.; Gorman, C. B.; Gilmour, S.; Biddle, S. L.; Bourhill, G. *J. Am. Chem. Soc.* **1993**, *115*, 2524−2526.
(9) Meyers, F.; Marder, S. R.; Pierce, B. M.; Brédas, J.-L. *J. Am. Chem. Soc.* **1994**, *116*, 10703−10714.
(10) Boxer, S. G. In *The Photosynthetic Reaction Center*; Deisenhofer, J., Norris, J. R., Eds.; Academic Press: San Diego, 1993; pp 179−220.
(11) Reichardt, C. *Solvents and Solvent Effects in Organic Chemistry*, 2nd ed.; VCH: Weinheim, 1988, and references therein.

S0002-7863(96)04081-4 CCC: $14.00

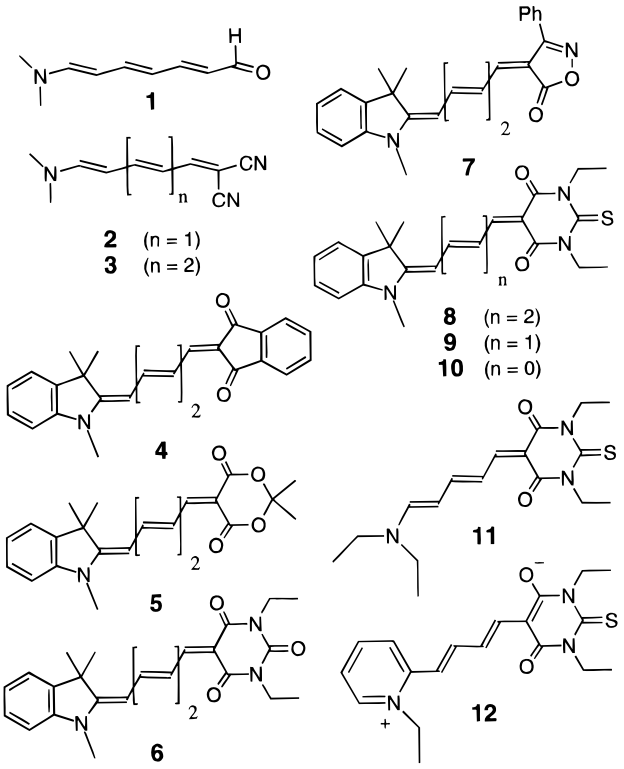

Figure 1. Structures of the studied donor/acceptor polyenes. All compounds are represented as if they adopted an electronic structure similar to limit **A**, except for **12** where the true ground state structure is believed to be closer to limit **E** (see text).

changing solvent. Describing the effects of both the donor and acceptor end groups and the solvent as due to the influence of an internal or matrix electric field allows for the integration of the two effects, and it is then also possible to connect them to theoretical descriptions of the linear and nonlinear electronic parameters of these molecules.[7,9,12]

Electroabsorption or Stark spectroscopy probes the electronic structure of a molecule by looking at the effect of an *externally applied* electric field on its absorption spectrum. The magnitude of the externally applied field is relatively weak compared to the internal or solvent-induced fields described above. In contrast to Stark spectroscopy of liquid samples, Stark spectra of frozen, immobilized samples have no contribution from the reorientation of the molecules in the applied field, which depends on the ground state dipole moment, but only from the changes in electronic structure associated with an optical transition. We report spectra for a series of donor/acceptor substituted polyenes whose structures are shown in Figure 1. All of these compounds exhibit a very intense absorption in the visible region of the spectrum and show moderate to extremely large electrooptical responses.

Experimental Section

The setup used for recording Stark spectra has been described in detail elsewhere.[10] In brief, light from a 250-W tungsten−halogen lamp was passed through a 0.22-m single monochromator (SPEX 1681), horizontally polarized using a Glan-Thompson polarizer, focused through the sample and detected with an amplified Si-photodiode detector. The spectral resolution of the setup was about 1.7 nm in the region studied.

Stark sample cuvettes were fabricated from ITO-coated (1700 Å) glass slides, glued together with Ablefilm 539IA mylar spacers (Ablestik Laboratories) with a nominal thickness of 25 μm. The thickness of these cuvettes was measured interferometrically at room temperature and was typically between 25 and 30 μm. With a thermal expansion coefficient of the spacer material of <100 ppm/°C this thickness should change by <0.75 μm upon going to liquid nitrogen temperature. The sample is open to the environment on two sides to allow the solution to contract upon freezing without affecting the sample thickness. An AC electric field was supplied by a custom-built high-voltage power supply, which amplified an externally supplied, digitally generated sinusoidal voltage. Samples were immersed in liquid nitrogen in a dewar fitted with strain-free quartz windows. The angle χ between the applied field direction and the electric vector of the polarized light (horizontal) was varied by rotating the sample about the vertical axis. The accuracy of this angle adjustment was ±5°. Helium gas was blown over the surface of the liquid nitrogen to prevent bubbling. The Stark signal (ΔI) was recorded with a lockin amplifier (Stanford Research Systems SRS850) detecting at the second harmonic of the applied external field. The direct output voltage of the Si-photodiode (I) was recorded as well so that the change in absorption of the sample due to the externally applied field could be calculated as $\Delta A \cong (2\sqrt{2}/\ln 10)\cdot(\Delta I/I)$. Absorption spectra were taken on the same setup as the Stark spectra as well as on a Varian 2300 spectrophotometer. Both gave identical spectra.

The compounds were synthesized as described in the literature.[2,3,13] Samples were dissolved in 2-methyltetrahydrofuran (2-MeTHF) at a concentration of about 1 mM. For compounds **2**, **3**, **4**, and **8**, additional Stark spectra were taken at about 20- to 100-fold higher dilution. For compounds **4** and **8** the experiments were also performed with solutions in frozen toluene and ethanol (EtOH).

Methods of Analysis

For an immobilized, isotropic sample the Stark spectrum can be described as the sum of the zeroth (amplitude change), first (band shift), and second (band broadening) derivative of the absorption spectrum, which in turn are related to changes in the transition moment upon application of an external field and the changes in polarizability $\underline{\Delta\alpha}$ and dipole moment ($\Delta\vec{\mu}$) upon transition from ground to excited state, respectively.[14−16]

$$\Delta A(\bar{\nu}) = F^2\left\{A_\chi A(\bar{\nu}) + \frac{B_\chi}{15hc}\bar{\nu}\frac{\mathrm{d}}{\mathrm{d}\bar{\nu}}\left(\frac{A(\bar{\nu})}{\bar{\nu}}\right) + \frac{C_\chi}{30h^2c^2}\bar{\nu}\frac{\mathrm{d}^2}{\mathrm{d}\bar{\nu}^2}\left(\frac{A(\bar{\nu})}{\bar{\nu}}\right)\right\} \quad (1)$$

with

$$A_\chi = \frac{1}{30|\vec{m}|^2}\sum_{ij}[10A_{ij}^2 + (3\cos^2\chi - 1)(3A_{ii}A_{jj} + 2A_{ij}^2)] + \frac{1}{15|\vec{m}|^2}\sum_{ij}[10m_iB_{ijj} + (3\cos^2\chi - 1)(4m_iB_{ijj})] \quad (2)$$

$$B_\chi = \frac{5}{2}\mathrm{Tr}(\underline{\Delta\alpha}) + (3\cos^2\chi - 1)\left(\frac{3}{2}\underline{\Delta\alpha}_m - \frac{1}{2}\mathrm{Tr}(\underline{\Delta\alpha})\right) + \frac{1}{|\vec{m}|^2}\sum_{ij}[10m_iA_{ij}\Delta\mu_j + (3\cos^2\chi - 1)(3m_iA_{jj}\Delta\mu_i + m_iA_{ij}\Delta\mu_j)] \quad (3)$$

$$C_\chi = |\Delta\mu|^2[5 + (3\cos^2\chi - 1)(3\cos^2\zeta_A - 1)] \quad (4)$$

where A and B are the transition polarizability and transition hyperpolarizability, respectively, reflecting the influence of the electric field on the transition moment $\vec{m}$: $\vec{m}(F) = \vec{m} + \underline{A}\cdot\vec{F} + \vec{F}\cdot\underline{\underline{B}}\cdot\vec{F}$. χ is the experimental angle between the externally applied field and the polarization of the incident light, ζ_A is the angle between $\Delta\vec{\mu}$ and the transition moment, and $\underline{\Delta\alpha}_m$ is the component of the polarizability

(12) Gorman, C. B.; Marder, S. R. *Chem. Mater.* **1995**, *7*, 215−220.
(13) Scheibe, P.; Schneider, S.; Dörr, F.; Daltrozzo, E. *Ber. Bunsen-Ges. Phys. Chem.* **1976**, *80*, 630−638.
(14) Liptay, W. In *Excited States*; Lim, E. C., Ed.; Academic Press: New York, 1974; pp 129−229.
(15) Mathies, R. A. Ph.D. Thesis, Cornell University, 1974.
(16) Bublitz, G. U.; Boxer, S. G. *Annu. Rev. Phys. Chem.* In press.

Table 1. Spectroscopic Properties of the Absorption Spectra and Results of the Analysis of the ΔA (Stark) Spectra for the Studied Compounds

							main absorption band			vibronic side band		
compd	solvent	pK_A[a]	$\bar{\nu}_{max}$[b] [cm^{-1}]	$\bar{\nu}_{1/2}$[c] [cm^{-1}]	$\Delta\bar{\nu}_{side}$[d] [cm^{-1}]	A_{side}[e] [%]	A_χ[f] [10^{-20} m^2/V^2]	$\Delta\alpha\cdot f^2$ [Å^3]	$\lvert\Delta\mu\rvert\cdot f$ [D]	A_χ[f] [10^{-20} m^2/V^2]	$\Delta\alpha\cdot f^2$ [Å^3]	$\lvert\Delta\mu\rvert\cdot f$ [D]
1	2-MeTHF	14.5	22 170	1100[g]	1020	97	-10 ± 2	550 ± 100	10.0 ± 1.0	-6 ± 2	135 ± 25	11 ± 1.0
2	2-MeTHF	11.2	20 720	800	1130	33	-3.5 ± 0.5	-120 ± 35	1.6 ± 0.2	4 ± 2	-235 ± 50	1.0 ± 0.2
3	2-MeTHF	11.2	17 070	650	1170	22	-15 ± 5	-165 ± 50	2.6 ± 0.3	20 ± 5	-435 ± 85	3.7 ± 0.3
4	toluene	7.1	14 800	900	1220	53	-10 ± 5	1900 ± 300	14.0 ± 1.0	15 ± 10	500 ± 100	15.8 ± 1.0
4	2-MeTHF		14 440	750	1270	27	-20 ± 8	1000 ± 170	10.0 ± 0.5	70 ± 20	185 ± 35	13.5 ± 0.5
4	EtOH		14 150	500	1280	17	-45	-50	2.5	*h*	*h*	*h*
5	2-MeTHF	5.1	15 300	700	1290	23	-25 ± 5	300 ± 85	6.2 ± 0.5	70 ± 20	150 ± 85	9.8 ± 0.5
6	2-MeTHF	4.6[i]	14 890	750	1280	23	-55 ± 20	385 ± 85	6.0 ± 0.6	65 ± 20	165 ± 85	10.2 ± 1.0
7	2-MeTHF	4.0	14 520	650	1210	32	-30 ± 10	300 ± 85	5.4 ± 0.6	25 ± 10	-350 ± 85	8.1 ± 0.8
8	toluene	2.5[i]	14 450	675	1260	31	-15 ± 5	600 ± 120	8.0 ± 0.8	30 ± 10	-335 ± 65	10.9 ± 1.0
8	2-MeTHF		14 270	500	1240	16	-25 ± 10	-300 ± 50	2.0 ± 0.2	50 ± 10	-735 ± 135	3.6 ± 0.4
8	EtOH		14 390	675	1330	36	-17	325	0	*h*	*h*	*h*
9	2-MeTHF	2.5[i]	16 740	450	1220	21	-10 ± 5	-165 ± 35	1.8 ± 0.2	20 ± 10	-250 ± 50	3.0 ± 0.3
10	2-MeTHF	2.5[i]	19 990	350[g]	1220	52	1 ± 0.5	-40 ± 10	2.0 ± 0.2	0.5 ± 0.5	-25 ± 15	2.7 ± 0.3
11	2-MeTHF	2.5[i]	18 960	800	1260	35	-7 ± 3	85 ± 15	3.8 ± 0.4	6 ± 3	-150 ± 35	5.6 ± 0.6
12	2-MeTHF	2.5[i]	18 080	1000[g]	1240	78	-12 ± 3	800 ± 170	12.0 ± 1.0	-5 ± 5	135 ± 25	12.8 ± 1.0

[a] pK_A value of the free acceptor end group. These values were obtained from a search of the Beilstein database. [b] Absorption maximum. [c] Full width at half maximum for the main absorption peak. [d] Spacing of the side band maximum with respect to the position of the main peak. [e] Relative intensity of the vibronic side band compared to the main peak. [f] For an experimental angle $\chi = 90°$. [g] Estimated from the model of the absorption spectrum. [h] Agreement between model and data is not good enough in this region to yield reliable numbers. [i] pK_A of the dimethyl form.

change along the direction of the transition moment (i.e., $\Delta\alpha_m = (\vec{m}\underline{\Delta\alpha}\vec{m})/|\vec{m}|^2$). The indices *i*,*j* are used for individual components of the vectors/tensors and run over the coordinates *x*, *y*, *z*. Decomposition of the ΔA spectrum into absorption derivative components yields values for A_χ, B_χ, and C_χ, which then can be used to extract information on the molecular parameters.

For a charge-transfer transition involving both the donor and acceptor group at opposite ends of the polyene bridge, the angle ζ_A between the direction of the transition moment $\vec{m}$ and the direction of the difference dipole $\Delta\vec{\mu}$ is expected to be close to 0°. If the line shape of the ΔA spectrum is dominated by a second derivative contribution, ζ_A can be obtained directly by measuring the intensities of the Stark signal at different angles χ (eq 4). After correcting χ using Snell's law[17] and adjusting the Stark data for the increased path length as χ increases, the results for all data sets with dominant second derivative line shapes gave a value of $\zeta_A \approx 0°$ and $|\Delta\mu|$ was calculated directly using eq 4 (the values in Table 1 are for $\Delta\vec{\mu}||\vec{m}$, i.e., $\zeta_A = 0°$).[18] It is evident from eq 4 that we can obtain information on the magnitude of $\Delta\mu$ directly from the second derivative contribution to the Stark line shape, but not on its sign. As discussed below, in some cases we may be able to infer the sign from other arguments. The first derivative term has contributions from two different origins. If one neglects the cross terms between the transition polarizability $\underline{A}$ and $\Delta\vec{\mu}$ (see below), this component is only related to the change in polarizability $\Delta\alpha$ associated with the electronic transition. Furthermore, it seems reasonable, for the same reasons as stated above, to assume that the main contribution to $\underline{\Delta\alpha}$ lies along the direction of the transition moment.[19] With these assumptions the first derivative component becomes linearly related to the change in polarizability: $B_\chi = {}^3/_2\Delta\alpha$. For $\Delta\alpha$, one can obtain information on both the sign (from the direction of the shift of the first derivative contribution) and magnitude. The zeroth derivative term also has contributions from two different origins—the transition polarizability $\underline{A}$ and the transition hyperpolarizability $\underline{\underline{B}}$. In many cases good agreement between the data and the best fit can be reached with just a sum of first and second derivative components, and thus the zeroth derivative component often can be neglected. However, for most of the compounds studied here good fits could only be obtained if a zeroth derivative component was included. In Table 1 we report the raw fitting parameter A_χ since the contributions from $\underline{A}$ and $\underline{\underline{B}}$ cannot be distinguished from the experimental data.

ΔA spectra were fit to the zeroth and $\bar{\nu}$-weighted first and second derivatives of the absorption spectra. These derivatives can be obtained in two different ways. Direct numerical differentiation of the absorption spectrum requires smoothing of the data prior to taking the derivative in order to decrease the noise level of the derivative. Typically a [10,10,3]-Savizky-Golay filter gave good results with minimal depression of peak values. Alternatively, the absorption spectra were fit to a sum of Gaussian bands whose analytical derivatives were then used to model the ΔA spectrum. A total of 4 or 5 Gaussian bands gave very good results with residuals typically less than 0.5%. Both approaches gave identical results in the subsequent analysis. In general, when multiple Gaussian components are used these are simply a general fitting function, so there is no physical meaning to the components. In some cases, however, where multiple absorption bands are present, this can also be used as a deconvolution strategy. For example, different vibronic transitions may exhibit different electrooptic properties.[20] The approach of fitting to multiple Gaussian bands also allows one to model the ΔA spectrum for a single band with more than one set of parameters (for example the values of A_χ, B_χ, and C_χ may vary across the inhomogeneous absorption band), and it does not require any smoothing of the data prior to analysis.

Many of the strong transitions observed here exhibit some resolved vibronic structure at 77 K, and in these cases the ΔA spectra were also fit to a combination of two parameter sets, one set for each absorption feature. Since the transitions overlap to some extent, care has to be taken not to produce artificial values due to interfering effects on the two bands (ΔA for each can be either positive or negative).[21] This was achieved by fixing the parameter values resulting from a one-parameter set fit, which mainly modeled the main absorption band and its accompanying ΔA signal, while allowing the parameter set for the vibronic band to vary. While this method cannot completely eliminate

(17) $n_1 \sin\theta_1 = n_2 \sin\theta_2$, where n_1 and n_2 are the refractive indices of the liquid nitrogen ($n_1 = 1.205$) and of the sample and θ_1 is the externally set experimental angle, $\theta_2 = 90° - \chi$. The refractive index of frozen 2-MeTHF could not be found in the literature. It is quite different from that of liquid 2-MeTHF ($n = 1.4059$ at room temperature) and was determined in two different ways. A refractive index of 1.8 ± 0.1 was determined for the frozen 2-MeTHF glass from the ratio of the sample's absorption at $\theta_1 = 0°$ and 40° and application of Snell's law. Alternatively, the refractive index can be calculated by measuring the capacitance of the empty cell and sample-filled cell. Correcting both for the capacitance of the sample holder using $n = \epsilon^{1/2} = [(C_{sample} - C_{holder})/(C_{empty} - C_{holder})]^{1/2}$ a value of 1.80 ± 0.05 was obtained.

(18) The calculated values of $|\Delta\mu|$ are not very sensitive to small deviations from $\zeta_A = 0°$. Angles as large as $\zeta_A = 20°$ would only lead to a decrease of the extracted $|\Delta\mu|$ values by about 5%, which is well within experimental errors.

(19) Ponder, M.; Mathies, R. *J. Phys. Chem.* **1983**, *87*, 5090−5098.

(20) Wortmann, R.; Elich, K.; Liptay, W. *Chem. Phys.* **1988**, *124*, 395−409.

(21) A combination of positive and negative zeroth derivatives for the main and side band, respectively, can create an artificial overall first derivative line shape. Likewise a combination of positive and negative first derivatives can create an artificial overall second derivative line shape.

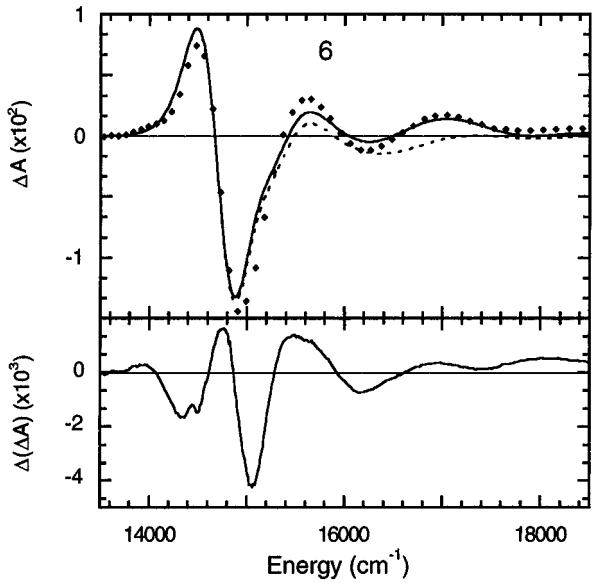

Figure 2. Stark spectrum (◆) and fits using one-parameter set (···) and two parameter sets (—) for compound **6** in frozen 2-MeTHF. This represents the case with the largest deviation between data and fit using 2-MeTHF or toluene as solvent. The data were taken in a continuous scan and only some points are shown so that both data and fit can be seen clearly. The bottom panel shows the residuals of the two parameter set fit.

residual contributions of the vibronic band to the electrooptic parameters of the main absorption band, it minimizes artifacts due to interference.

The experimental errors of the results in Table 1 are due to two main sources: errors in determining the magnitude of both the electric field and the sample's absorption. There is uncertainty in the exact magnitude of the electric field strength felt by the molecule as there is a difference between the externally applied field and the internal field at the position of the molecule. The internal field $\vec{F}$ whose magnitude enters into eq 1 can be expressed as: $\vec{F} = \mathbf{f}\cdot\vec{F}_{ext}$, where **f** is a tensor describing the local field correction[22] and $\vec{F}_{ext}$ is the externally applied field. The applied voltage is known accurately; the sample thickness is a source of error, though this is likely systematic as any shrinkage is identical in different samples. The parameters in Table 1 are given in terms of **f** to emphasize that this additional factor has not been determined experimentally. Both A_χ and $\Delta\alpha$ depend quadratically on the field strength and linearly on the sample's absorbance while $\Delta\mu$ depends linearly on F and on the square root of the sample's absorbance leading to the smaller relative errors for the reported values for $\Delta\mu$. Further sources of error associated with the method are found in the Discussion section.

Results

All Stark spectra shown in Figures 2−7 were taken at $\chi = 90°$ and were scaled to a peak absorption of unity and an external electric field of 1×10^6 V/cm to ease comparison among different compounds. As predicted by eq 1, ΔA scaled quadratically with the applied field. The absorption spectra of compounds **1**−**12** exhibit an intense peak in the visible region accompanied by another clearly resolved peak typically 1200−1300 cm^{-1} at higher energy and a less resolved, but still distinguishable, shoulder at roughly the same spacing to higher energy. The width of the main peak and the relative intensities of the vibronic side bands vary from compound to compound. These absorption results are summarized in Table 1. As discussed above, although vibronic structure is an expected feature in the electronic spectra of these compounds, this structure greatly complicates the analysis of the Stark spectra as the electrooptic parameters may be different for different vibronic features. A worst case example of this is illustrated in Figure 2 which shows the Stark data for compound **6** and the one-parameter-set and two-parameter-set fits to the Stark data. The one-parameter-set fitting gives good results for the main band of the ΔA spectrum located at the same energy as the main absorption peak, but only moderate agreement with the ΔA accompanying the vibronic side band at higher energy. Allowing for a second set of Stark parameters as described above led to greatly improved fits as shown. For all other data sets with 2-MeTHF or toluene as solvent, the agreement between data and fit is at least as good as that shown in Figure 2, but usually much better. The results of these fits and of those for the other compounds discussed below are presented in Table 1.

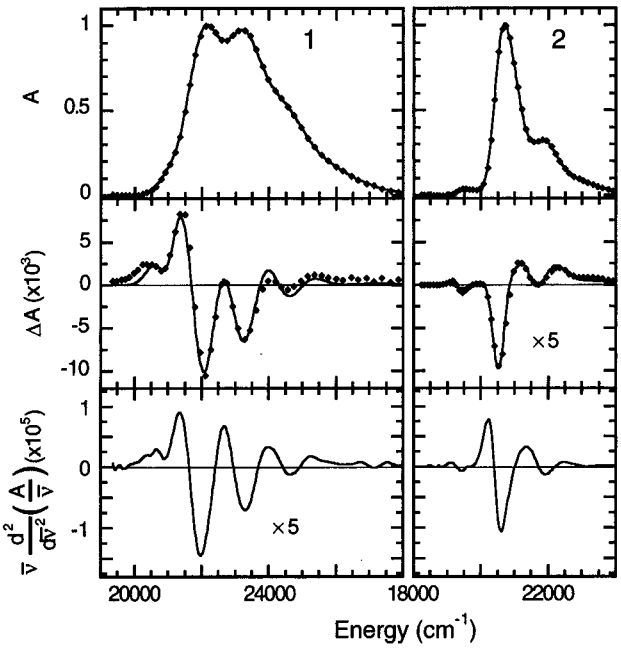

Figure 3. Absorption spectra (top panels), ΔA (Stark) spectra (center panels), and $\bar{\nu}$-weighted second derivatives of the absorption spectra (bottom panels) for **1** and **2** in frozen 2-MeTHF. For the absorption and ΔA spectra both data (◆) and fit (—) are shown. All spectra were scaled to a peak absorbance of unity and a field strength of 1×10^6 V/cm to facilitate comparisons. The ΔA spectrum of **2** and the second derivative of **1** were multiplied by a factor of 5 to increase visibility of the data.

Stark Spectra in 2-MeTHF. The absorption spectrum of **1** (top left panel, Figure 3) exhibits an especially broad main peak along with a vibronic side band of nearly equal intensity. The ΔA spectrum (center left panel, Figure 3) shows an overall second derivative line shape (compare with the second derivative of the absorption in the lower left panel of Figure 3) which translates into a rather large difference dipole moment of $|\Delta\mu| = 10$ D.[23] The fitting procedure also reveals a considerable first derivative contribution which yields a change in polariz-

(22) f depends on the dielectric constant (ϵ) of both the solvent and the solute. A quite realistic approach is to model f by an ellipsoidal dielectric imbedded within another dielectric [Böttcher, C. J. F. *Theory of Electric Polarization*, 2nd ed.; Elsevier: Amsterdam, 1973; Vol. 1, p 79ff]. For the frozen 2-MeTHF matrix ϵ can be estimated from capacitance measurements (15) to be about 3.2. ϵ is unknown for the studied molecules, but should be close to the same value. Using appropriate molecular dimensions of 20 Å × 4 Å × 4 Å and a rather large range of ϵ between 5.5 and 2 for the studied compounds, the local field correction would be 0.75−1.22 along the short molecular axis and 0.96−1.02 along the long axis. Since the main components of both $|\Delta\mu|$ and $\Delta\alpha$ lie along the long molecular axis (see text) the local field correction factor will be neglected in the discussion.

(23) In calculating $|\Delta\mu|$, the ratio of ΔA and the second derivative of the absorption spectrum has to be evaluated. Since a broad absorption spectrum gives rise to a rather small second derivative both have to be considered in order to extract molecular parameters.

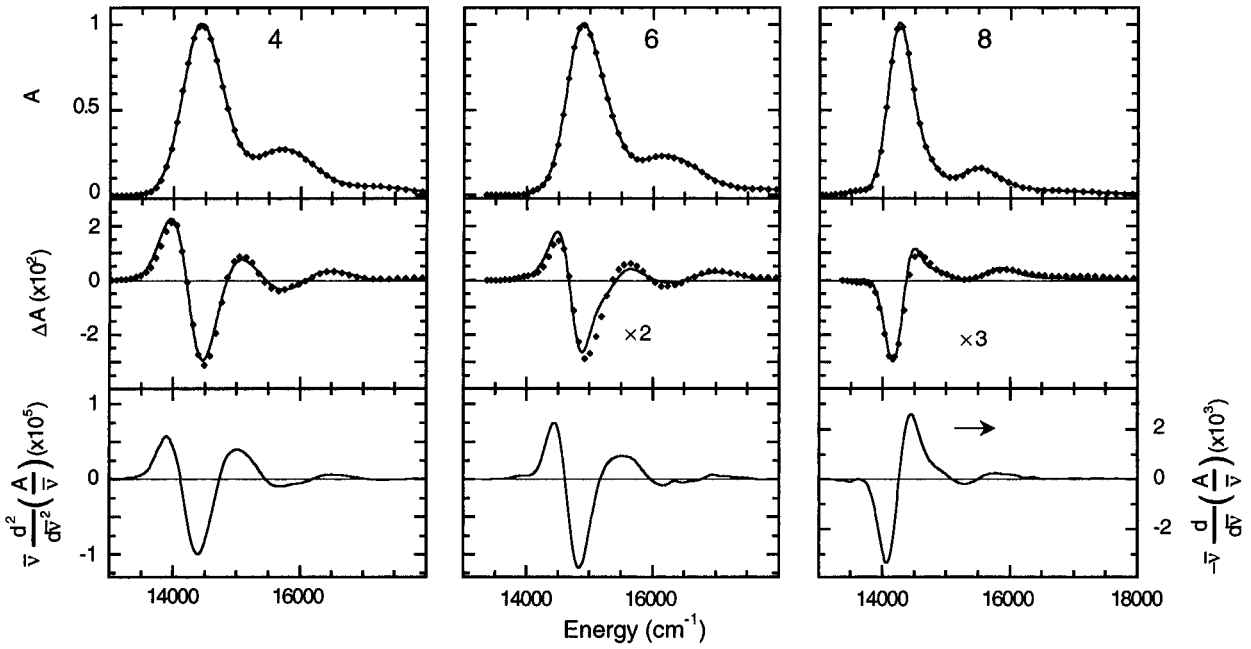

Figure 4. Acceptor dependence of the absorption spectra (top panels), ΔA (Stark) spectra (center panels) and $\bar{\nu}$-weighted derivatives of the absorption spectra (bottom panels) for **4**, **6** and **8** in frozen 2-MeTHF. For **4** and **6** the second derivative is shown, for **8** the negative first derivative. For the absorption and ΔA spectra both data (◆) and fit (—) are shown. All spectra were scaled to a peak absorbance of unity and a field strength of 1×10^6 V/cm to facilitate comparisons. The ΔA spectra for **6** and **8** were multiplied by a factor of 2 and 3, respectively, to increase visibility of the data.

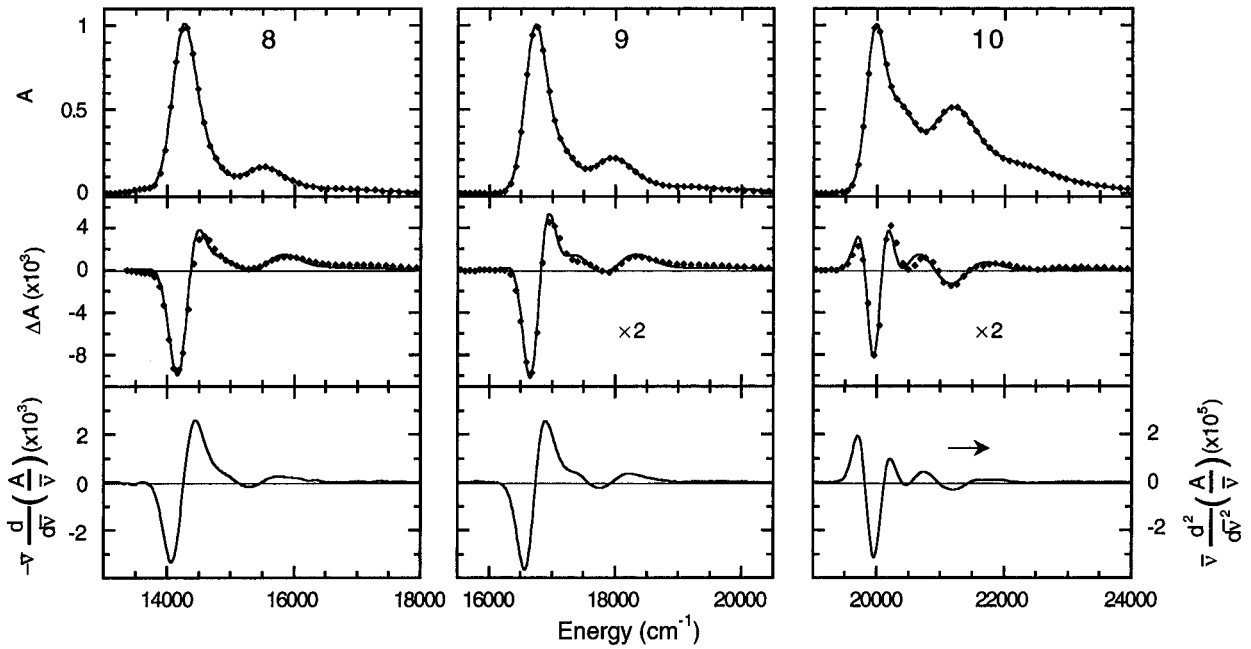

Figure 5. Chain length dependence of the absorption spectra (top panels), ΔA (Stark) spectra (center panels), and $\bar{\nu}$-weighted derivatives of the absorption spectra (bottom panels) for **8**, **9**, and **10** in frozen 2-MeTHF. For **8** and **9** the negative first derivative is shown, for **10** the second derivative. For the absorption and ΔA spectra both data (◆) and fit (—) are shown. All spectra were scaled to a peak absorbance of unity and a field strength of 1×10^6 V/cm to facilitate comparisons. The ΔA spectra for **9** and **10** were multiplied by a factor of 2 to increase visibility of the data.

ability of $\Delta\alpha = +550$ Å^3. The parameters for the vibronic band differ from those of the main band to some extent: $|\Delta\mu|$ is only slightly larger, while $\Delta\alpha$ is smaller by a factor of about 4. The best fit (shown superimposed on all A and ΔA spectra) matches the data quite well in the region of the two main peaks. At the low-energy edge around 20 500 cm^{-1} a positive feature can be observed in the ΔA spectrum which, while also present in the second derivative of the absorption spectrum, is underestimated in the best fit.[24] At energies above 23 000 cm^{-1} in the region of the shoulder in the absorption band, the fit overestimates the magnitude of the ΔA spectrum, but reproduces its curvature.

The spectra for **2** (Figure 3) and **3** (data not shown) are of very similar shape. The analysis of the ΔA spectra yields $|\Delta\mu| \approx 2$ D and $\Delta\alpha \approx -150$ Å^3 for both. A weak peak centered at 19 500 cm^{-1} is observed in the absorption spectrum of **2** at lower energy than the main absorption band. The accompanying Stark signal does not match the fit which otherwise models the ΔA spectrum very well. The same phenomenon is observed for **3.** The relative magnitude of these low-energy features increases with increasing sample concentration. Their origin might be the formation of aggregates since ΔA spectra at higher dilution

(24) Similar but less pronounced low-energy features are observed in the ΔA spectrum of **5**, **6**, and **7**.

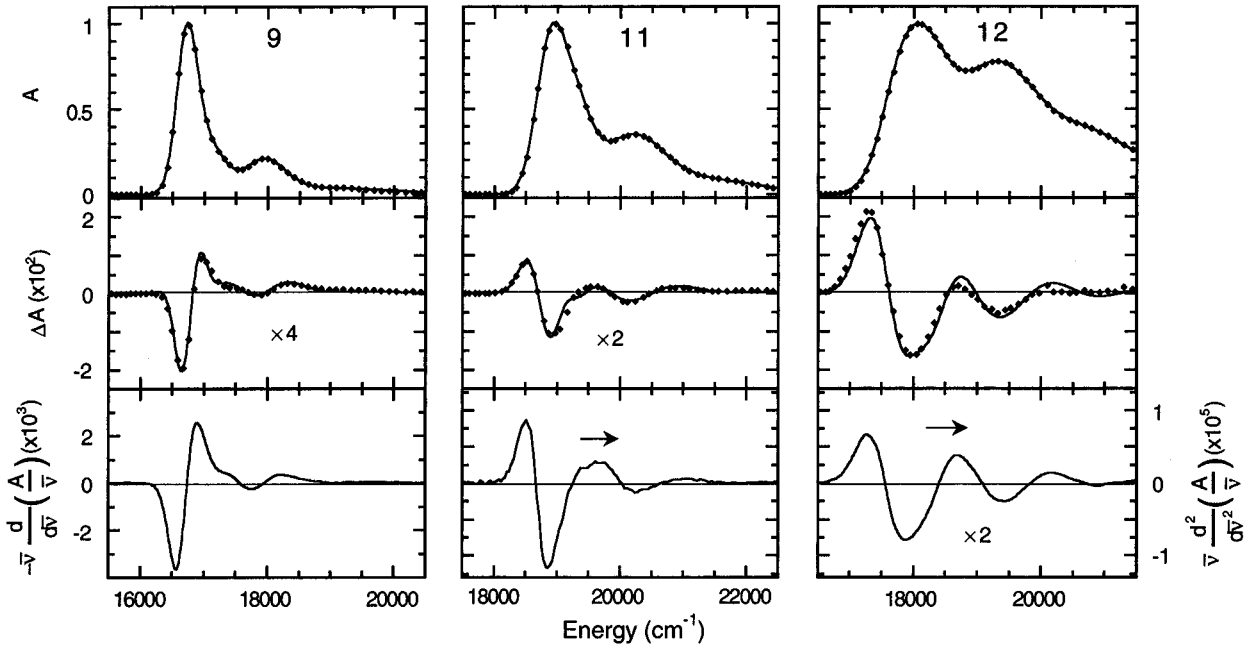

Figure 6. Donor dependence of the absorption spectra (top panels), Δ*A* (Stark) spectra (center panels), and $\bar{\nu}$-weighted derivatives of the absorption spectra (bottom panels) for **9**, **11**, and **12** in frozen 2-MeTHF. For **9** the negative first derivative is shown, for **11** and **12** the second derivative. For the absorption and Δ*A* spectra both data (◆) and fit (—) are shown. All spectra were scaled to a peak absorbance of unity and a field strength of 1×10^6 V/cm to facilitate comparisons. The Δ*A* spectrum for **9** was multiplied by a factor of 4, and the Δ*A* spectrum for **11** and the second derivative of **12** were multiplied by a factor of 2 to increase visibility of the data.

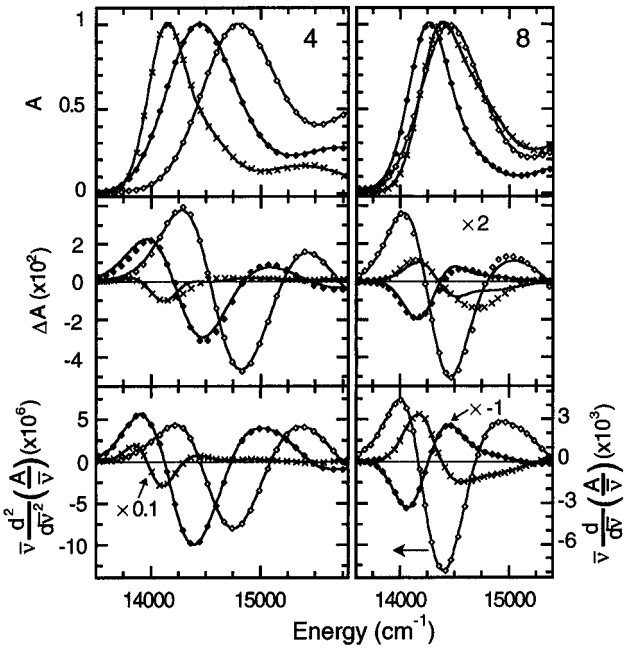

Figure 7. Solvent dependence of the absorption spectra (top panels), ΔA (Stark) spectra (center panels), and $\bar{\nu}$-weighted derivatives of the absorption spectra (bottom panels) for **4** and **8** in frozen EtOH, 2-MeTHF, and toluene. For **4** and **8** (toluene) the second derivative is shown, for **8** (EtOH) the first derivative, and for **8** (2-MeTHF) the negative first derivative. For the absorption and ΔA spectra both data (×, EtOH; ◆, 2-MeTHF; and ◇, toluene) and the fit (—) are shown. The derivatives are labeled using the same symbols. All spectra were scaled to a peak absorbance of unity and a field strength of 1×10^6 V/cm to facilitate comparisons. Δ*A* spectra for **8** were multiplied by a factor of 2. The derivative for **4** in EtOH was divided by a factor of 10 to increase visibility of the other data.

for both **2** and **3** show signals with a very small low-energy feature but an otherwise identical (though noisier) line shape. These additional absorption peaks, which are only observed at low temperature, have been previously assigned to the presence of dimers.[25] Qualitatively, the Δ*A* signal of this transition is larger than the monomer's signal, and for **2**, where this band is better separated, we estimate $|\Delta\mu|$ to be about 1.5 times larger than for the monomer. A more quantitative analysis is not possible as this would require more information on the dimer's absorption line shape. Another possible source of additional absorption peaks would be the presence of different isomers. Although the absorption spectra of the cis isomers of **2** and **3** have been predicted to be slightly red shifted,[13] they are less stable than the all-trans form[13,26] and thus would only be present in minute amounts and not affect the observed Δ*A* spectra.

Compounds **4** through **8** have the same donor and polyene spacer, but differ in the acceptor end group. The absorption spectra of **4**, **5**, and **6** are quite similar in peak position and width as well as relative intensity of the vibronic side band. Compounds **7** and **8** show a narrower main peak and a vibronic band of different intensity (*cf.* Table 1). Figure 4 shows representative spectra for three of these compounds, **4**, **6**, and **8**. The Δ*A* spectra for compounds **4**−**7** all show a dominant second derivative line shape, while the Δ*A* spectrum for **8** is very different, being dominated by a negative first derivative line shape. Analysis of the Δ*A* spectrum for compound **4** gives $|\Delta\mu| = 10$ D and $\Delta\alpha = +1100$ Å^3; while compounds **5**−**7** have similar values of $|\Delta\mu| \approx 6$ D and $\Delta\alpha \approx +340$ Å^3. For compound **8** $|\Delta\mu| = 2$ D and $\Delta\alpha = -300$ Å^3. For **4**−**7** the best fit slightly overestimates the main positive peak at the low-energy side of the Δ*A* spectrum while underestimating the main negative peak. This deviation amounts to a maximum of about 5% in the case of **4,** about 10% for **5,** and 20% for **6** and **7**. At the same time the fits for the higher energy side band become less accurate. The largest residual is located in the region between the main negative peak of the Δ*A* spectrum and the

(25) Berdyugin, V. V.; Vasileva, I. A.; Galanin, M. D.; Krasnaya, Z. A.; Nikitina, A. N.; Chizhikova, Z. A. *Opt. Spectrosc. (USSR)* **1987**, *63*, 38−40.

(26) Joerges, E.; Schneider, S.; Dörr, F.; Daltrozzo, E. *Ber. Bunsen-Ges. Phys. Chem.* **1976**, *80*, 639−645.

(27) The same phenomenon, although less pronounced, can also be observed for **3**, **8**, **9**, and **10**.

next positive peak toward higher energy (*cf.* Figure 2).[27] Nevertheless, the results of the analysis show consistently for all four compounds an increased value of $|\Delta\mu|$ as well as a decreased value of $\Delta\alpha$ for the side band, compared to the main band. The best fit maps the data very well for compound **8**. The ΔA spectra of **4** and **8** at higher dilution had identical line shapes as the more concentrated samples (data not shown).

Compounds **9** and **10** have the same donor and acceptor end groups as **8**, but the linking polyene bridge is shorter by two and four C atoms, respectively. The absorption and Stark spectral shape of **9** is very similar to that of **8** (Figure 5), but ΔA for **9** is only about half of that for **8**, translating into a reduced magnitude of $\Delta\alpha = -165$ Å^3 ($|\Delta\mu|$ is unchanged). The absorption spectrum of compound **10** is quite different from **8** and **9** as the relative intensity of the higher energy vibronic band is considerably larger, the main peak is narrower, and there is a shoulder between these features at about 20400 cm^{-1}. The ΔA spectrum is dominated by a second derivative line shape with $|\Delta\mu| = 2$ D as for **8** and **9** but a substantially reduced magnitude of $\Delta\alpha = -40$ Å^3. The best fit maps the ΔA spectra quite well, except for **10** where a rather large deviation in the region around 20 500 cm^{-1} is observed.

Compounds **11** and **12** have a structure similar to **9** but different donor end groups. Unlike the ΔA spectrum of **9**, both **11** and **12** show a dominant second derivative line shape (Figure 6), translating into values for $|\Delta\mu|$ of about 4 and 12 D and $\Delta\alpha$ of about $+85$ and $+800$ Å^3, respectively. The fits model the ΔA spectra quite well for both compounds with the exception of **11** where a rather large residual of about 10% is observed in the same region as for **5**−**7**. The results of the analysis for the vibronic band are similar to those described above, showing increased values of $|\Delta\mu|$ as well as decreased values of $\Delta\alpha$ compared with the main peak.

Solvent Dependence. The polarity and molecular nature of the solvent affect both the absorption and Stark spectra of these compounds. This is illustrated with compounds **4** and **8**. The absorption spectrum of **4** is shown in the top left panel of Figure 7. The position of the main band shifts 350 cm^{-1} toward higher energy in frozen toluene and 300 cm^{-1} toward lower energy in frozen EtOH compared with frozen 2-MeTHF. At the same time the width of the main band and the relative intensity of the vibronic band change: both increase in toluene and decrease in EtOH. The change in the ΔA spectrum is even more pronounced (center left panel, Figure 7). The line shape is dominated by a second derivative contribution in all three solvents (see lower left panel, Figure 7); however, its magnitude varies strongly. In toluene the Stark signal is extremely large, and the best fit traces the ΔA spectrum very well yielding values of $|\Delta\mu| = 14$ D and $\Delta\alpha = +1900$ Å^3. In EtOH the ΔA spectrum is about tenfold weaker which, in combination with the about fourfold stronger second derivative of the absorption spectrum, yields $|\Delta\mu| = 2.5$ D. The value for $\Delta\alpha = -50$ Å^3 has changed dramatically too and is now negative. The agreement between the best fit and data is not as good as for the spectrum in toluene. The vibronic band's Stark signal is very weak and does not give reliable results in the fitting. Additionally there is a rather large residual in the fit of the ΔA spectrum in the region between the two peaks of the absorption.

The absorption spectrum of **8** also shows a strong influence of the solvent (top right panel, Figure 7). Here the changes are in the same direction for both toluene and EtOH relative to 2-MeTHF. The position of the main peak shifts toward higher energy (180 and 120 cm^{-1}, respectively) while both the width of the main peak and the intensity of the vibronic band increase significantly. The data for **8** in EtOH show a higher degree of noise than the other spectra due to the low solubility of **8** in EtOH. As observed for **4**, the ΔA spectra show very large changes as the solvent is changed (center right panel, Figure 7). For both toluene and EtOH the Stark spectrum changes from the negative first derivative lineshape it displays in 2-MeTHF (lower right panel, Figure 7). In toluene the ΔA spectrum has a clear second derivative line shape and the best fit, which maps the data very well, yields values of $|\Delta\mu| = 8$ D and $\Delta\alpha = +600$ Å^3. In EtOH on the other hand the Stark signal is weaker and the best fit cannot describe it well. The main peak seems to fit best to a nearly pure first derivative line shape, giving a value of $\Delta\alpha = +325$ Å^3, but as for **4** in EtOH, the fit has a dominant residual at a position in between the absorption's two peaks.

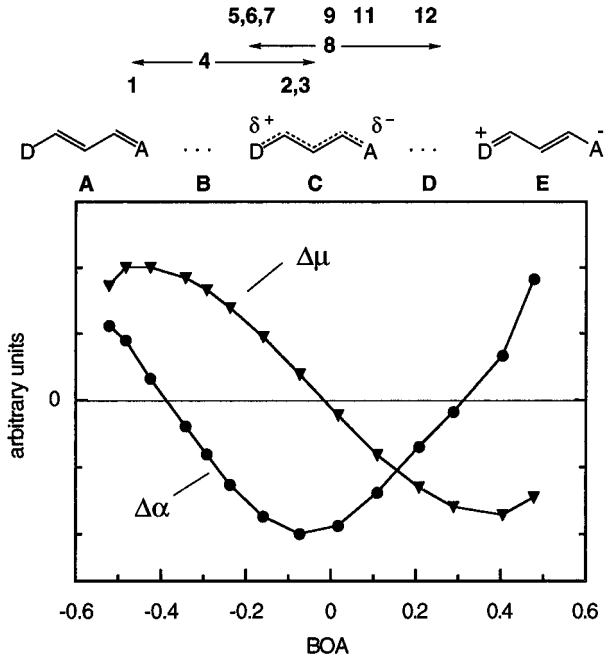

Figure 8. Predicted evolution of $\Delta\mu$ (▼) and $\Delta\alpha$ (●) with changing ground state structure (described by the degree of bond order alternation BOA) of donor/acceptor polyenes using the data from ref 9. The calculated data points are connected by lines in order to guide the eye. The position of the studied compounds between limits **A** and **E** (in a solvent matrix of frozen 2-MeTHF) as derived from comparison of the Stark data with the theoretical predictions is shown. For compounds **4** and **8** the approximate structural change upon changing the solvent to toluene (shift toward limit **A**) or EtOH (shift toward limit **E**) is indicated.

Discussion

General Trends. We discuss these results within the framework of the effects of the electron donating and accepting end groups on the connecting polyene bridge. The illustration introduced earlier is reproduced in Figure 8 with each compound placed on the **A**−**E** scale according to the analysis of the Stark data. In the case of compounds **4** and **8** which were studied as a function of solvent, the number is located at the approximate position found in 2-MeTHF, while the left and right ends of the arrows correspond to the ranges sampled by toluene and EtOH, respectively. These assignments were done by comparing the results obtained from the analysis of the Stark spectra with predicted values, as discussed below.

Several calculations have been reported in recent years exploring the dependence of the molecular electronic parameters (especially the hyperpolarizability β) on the ground state

structure (BOA or BLA) of donor/acceptor polyenes.[5,7,9,12,28−33] Although very different theoretical approaches were used, the predicted trends in the change of β with BOA are essentially the same and are in agreement with experimental results.[7,34−37] Since the information needed for the calculation of dipole moments μ and polarizabilities α is contained in these calculations of β, this agreement establishes confidence in the use of the expected trends in the changes of $\Delta\alpha$ and $\Delta\mu$ vs BOA for our assignments. Figure 8 shows this theoretically predicted evolution of the experimentally accessible parameters $\Delta\alpha$ and $\Delta\mu$ with changing ground state structure. Upon going from the fully localized structure **A** with very weak donor and acceptor groups toward a more perturbed bridge structure **B**, $\Delta\mu$ should increase as the transition gains more charge-transfer character. With increasing amount of delocalization in the ground state structure of the bridge, this trend should reverse because the ground state dipole moment increases along with the ground state delocalization of the bridge, and $\Delta\mu$ should thus get smaller. In the limit of case **C**, $\Delta\mu$ should be zero and will become negative for even stronger perturbation of the bridge before starting to reverse again toward smaller magnitudes as the ground state again approaches a fully localized, but now charge separated, structure (limit **E**). The situation for $\Delta\alpha$ is more subtle. $\Delta\alpha$ is expected to be large and positive for an unperturbed polyene and should decrease as the donor and/or acceptor gets stronger. At limit **C** the ground state exhibits maximum delocalization, hence maximum polarizability, and $\Delta\alpha$ should be negative, i.e., the polarizability of the excited state should be lower than that of the ground state. Upon further increase of the perturbation on the bridge, the polarizability of the ground state will decrease again, leading to an increase of $\Delta\alpha$ which should reach large positive values again toward limit **E**. The exact values of $\Delta\alpha$ and $\Delta\mu$ for a given donor/acceptor polyene will depend not only on its degree of BOA but also on additional factors such as the length of the polyene bridge and the chemical nature of the end groups. For chemically very similar compounds, however, these additional factors are expected to be about the same and the observed changes in $\Delta\alpha$ and $\Delta\mu$ should reflect differences in their relative position on the BOA scale, as outlined in Figure 8.

Acceptor Dependence (cf. Figure 4). Compounds **4**−**8** differ only in the electron accepting end group. The relative strength of the electron acceptor groups can be approximated by the acidity of the corresponding free end group at the position of its attachment to the polyene bridge. These pK_A values are listed in Table 1. The analysis of the Stark spectra for **4**−**8** in 2-MeTHF shows that with increasing acceptor strength the magnitudes of both $|\Delta\mu|$ and $\Delta\alpha$ decrease (*cf.* Table 1). This can be related to the theoretical predictions outlined above for the region spanned by structures **A**, **B**, and **C**. Compound **4** has a moderately strong acceptor end group and shows very large values of both $|\Delta\mu|$ and $\Delta\alpha$. Compound **5** has a considerably stronger acceptor, and the observed values of $|\Delta\mu|$ and $\Delta\alpha$ both decrease significantly. Compounds **6** and **7** have slightly stronger acceptors compared with **5**, and $|\Delta\mu|$ shows a trend toward smaller values, although the values are comparable within the experimental error. Within their experimental uncertainty the values of $\Delta\alpha$ are also similar for all three compounds. Compound **8** has a considerably stronger acceptor end group, and the values of both $|\Delta\mu|$ and $\Delta\alpha$ have decreased further; $\Delta\alpha$ is negative and dominates the electrooptic response. Based on these results in frozen 2-MeTHF compound **4** should be in the region of limit **B**, while **8** is close to **C**, and **5**, **6**, and **7** are in-between as illustrated in the upper part of Figure 8.

Donor Dependence (cf. Figure 6). Compounds **9**, **11**, and **12** differ only in the donor end group. Based on the results of the analysis of the Stark data, **9** has a very similar structure to **8**, i.e., it is close to the cyanine limit **C**. The ethylpyridinium end group of **12** is a very strong electron donor because it gains aromaticity upon loss of an electron. This gives credence to the view that the structure of **12** is close to the limit **D**, which would imply that its dipole moment is larger in the ground than in the excited state, i.e., $\Delta\mu = -12$ D. The values of both $|\Delta\mu|$ and $\Delta\alpha$ are small for **11** which places it, depending on the relative donor strength, either between **B** and **C** or between **C** and **D**. Based on the experimental results discussed below for compounds **1**−**3**, we believe that the diethylamine group in **11** is a stronger donor than the indole derivative in **9**. This electron withdrawing effect of the fused benzene ring which decreases the donor strength of the indole group can also be observed in the changed reactivities of small heterocyclic systems. In electrophilic substitution reactions the three simple condensed heterocycles (benzofuran, indole, benzothiophene) are markedly less reactive than the corresponding monocyclic heterocycle (furan, pyrrole, thiophene).[38] Thus we place **11** between **C** and **D**, implying that $\Delta\mu$ is negative.

Compounds 1−3 (cf. Figure 3). This set of simpler compounds can be viewed as model compounds for the class of donor/acceptor substituted polyenes. They have been well-studied both theoretically, especially in relation to their nonlinear optical properties,[12,39] and experimentally.[13,25,40] The data for **1** resemble those for **12** in showing a very broad absorption peak with an intense vibronic band, a large value of $|\Delta\mu| = 10$ D, and a moderately large $\Delta\alpha = +550$ Å^3. Because **1** has moderately strong donor and acceptor end groups, it is expected to be between limits **A** and **B**. Crystallographic data for **1**[8] show that the bond lengths in the bridge are closer to a polyene structure (limit **A**) than to a zwitterionic structure (limit **E**) as would be expected for **12**. Compounds **2** and **3** both have the same donor end group as **1**, but a different acceptor. Although they differ in the number of double bonds and carbon atoms in the bridge, analysis of the Stark spectra reveals very similar results for both: a small $|\Delta\mu| = 1.6$ and 2.6 D and a relatively small negative $\Delta\alpha = -120$ and -165 Å^3, respectively. Accordingly we place both **1** and **2** close to the cyanine limit **C**. This agrees with crystallographic data which show very small differences in the C−C bond lengths for **3**.[8] Based on these results we can also conclude that the dimethylamine end group in **1**−**3** is a stronger electron donor than the indole derivative in **4**−**8**, since both **2** and **3** show a stronger perturbation of the bridge than **4**−**7**, although the latter all have stronger acceptor end groups. A similar perturbation of the

(28) Albert, I. D. L.; Marks, T. J.; Ratner, M. A. *J. Phys. Chem.* **1996**, *100*, 9714−9725.
(29) Chen, G.; Mukamel, S. *J. Am. Chem. Soc.* **1995**, *117*, 4945−4964.
(30) Chen, G.; Mukamel, S. *J. Chem. Phys.* **1995**, *103*, 9355−9362.
(31) Chen, G.; Mukamel, S. *J. Phys. Chem.* **1996**, *100*, 11080−11085.
(32) Lu, D.; Chen, G.; Perry, J. W.; Goddard, W. A. *J. Am. Chem. Soc.* **1994**, *116*, 10679−10685.
(33) Dekhtyar, M. L.; Rozenbaum, V. M. *J. Phys. Chem.* **1995**, *99*, 11656−11658.
(34) Marder, S. R.; Beratan, D. N.; Cheng, L.-T. *Science* **1991**, *252*, 103−106.
(35) Ortiz, R.; Marder, S. R.; Cheng, L.-T.; Tiemann, B. G.; Cavagnero, S.; Ziller, J. W. *J. Chem. Soc., Chem. Commun.* **1994**, 2263−2264.
(36) Marder, S. R.; Gorman, C. B.; Tiemann, B. G.; Cheng, L.-T. *J. Am. Chem. Soc.* **1993**, *115*, 3006−3007.
(37) Bourhill, G.; Brédas, J.-L.; Cheng, L.-T.; Marder, S. R.; Meyers, F.; Perry, J. W.; Tiemann, B. G. *J. Am. Chem. Soc.* **1994**, *116*, 2619−2620.
(38) Streitwieser, A. J.; Heathcock, C. H. *Introduction to Organic Chemistry*; 3rd ed.; Macmillan: New York, 1985.
(39) Dehu, C.; Meyers, F.; Hendrickx, E.; Clays, K.; Persoons, A.; Marder, S. R.; Brédas, J.-L. *J. Am. Chem. Soc.* **1995**, *117*, 10127−10128.
(40) Baumann, W. *Z. Naturforsch.* **1983**, *38A*, 995−1002.

bridge structure is only obtained when the acceptor strength increases significantly, such as in **8**.

Chain Length Dependence. The results for compounds with similar donor and acceptor end groups but different lengths of the connecting bridge, such as **2** and **3** and **8**−**10**, yield information on the influence of the donor/acceptor separation on the molecular electronic structure. As already mentioned the results for **2** and **3** are quite similar, with **2** showing a slightly smaller value of $|\Delta\mu|$ than **3**, with $\Delta\alpha$ less negative. Similar results were obtained for **8**−**10** (*cf.* Figure 5). All three compounds show the same value of $|\Delta\mu| \approx 2$ D and $\Delta\alpha$ is negative, although its magnitude changes significantly. This is not sufficient data for a comprehensive description of the chain length dependence of the electronic structure since our results place all of these compounds in the same region, close to limit **C**. Nevertheless, it seems clear that the chain length does not greatly affect the degree of delocalization in the bridge and thus the ground state structure of the molecule.

Blanchard-Desce *et al.*[41] determined the dipole moment in both the ground and the excited state for two series of donor/acceptor substituted polyenes[42] containing $N = 1$, 2, 5, 7, and 9 double bonds in the polyene chain using electroabsorption spectroscopy in liquid dioxane. They report large values of $\Delta\mu$ for all compounds which would place them in the region between **A** and **B**, since both donor and acceptor groups are of moderate strength. For both series the ground state dipole moment remains constant regardless of chain length while the excited state dipole moment (and thus $\Delta\mu$) increases with increasing chain length.[43] For the longest studied chain ($N = 9$) this increase in $\Delta\mu$ levels off, possibly indicating a decrease in electronic coupling between the two end groups. Baumann measured electro-absorption spectra for **2** and **3** along with their analogs containing $N = 0$, 1, and 4 double bonds in the polyene chain in liquid solution, using three different solvents.[40] All of these (except for $N = 0$) exhibit large values of $\Delta\mu$ which strongly increase with increasing chain length, while the ground state dipole moment again does not change significantly.

Both of these studies thus indicate that in regions **A** and **B** too the ground state structure depends only slightly on the donor−acceptor separation. The changes in the magnitude of $\Delta\mu$ and $\Delta\alpha$ obtained for **2** and **3** and **8**−**10** accordingly mainly reflect differences in the length of the bridge but not in its degree of delocalization. A similar result was obtained in a recent theoretical study for $N = 2-7$ double bonds in the polyene bridge.[12] Nevertheless, in the two limiting cases this trend will break down. For very long chains the interaction between the end groups can be expected to decrease as indicated by the leveling off of the $\Delta\mu$ values for $N = 9$. On the other hand, for a very short bridge additional direct interactions of the donor and acceptor can be expected—this might be the case for compound **10**.

Solvent Effects. The ground state structure of donor/acceptor polyenes has been shown to depend on the polarity of the solvent.[40,44−46] The basic characteristics of this solvent dependence can also be understood within the same simple model shown in the top part of Figure 8. A nonpolar solvent will tend to decrease the ground state dipole moment of the solvated molecule while a polar solvent preferably stabilizes a dipolar ground state structure. Thus, a polar solvent should shift the structure closer to limit **E** while a nonpolar solvent will shift it closer to limit **A**. Along with these changes of the ground state structure, the excited state characteristics should change too. The observed solvent effect on the ΔA spectra of compounds **4** and **8** demonstrates that this indeed is the case and that these changes can be understood in the same picture as the influence of the donor and acceptor end groups. Upon changing the solvent from 2-MeTHF to the less polar toluene, compounds **4** and **8** exhibit an increase in both $|\Delta\mu|$ and $\Delta\alpha$, which is consistent with moving **4** to a point between **A** and **B** and **8** to a point between **B** and **C**. In other words, in toluene both compounds behave the same as another molecule with a weaker acceptor end group would in 2-MeTHF; for example, **8** in toluene resembles a molecule with an acceptor strength between that of **4** and **5** in 2-MeTHF. Changing the solvent to EtOH has the opposite effect, although now the situation is a little more complicated. Compound **4** now exhibits a Stark spectral signature of a molecule close to the cyanine limit **C**, i.e., a small $|\Delta\mu|$ and a negative value of $\Delta\alpha$. The agreement between data and fit, however, becomes poorer, and in the case of **8**, the best fit does not follow the ΔA spectrum very well. Qualitatively, the line shape indicates a dominant positive first derivative. This is also obtained from the fit; however, the fit has residuals of about 50% of the data's value in the region above 14 500 cm^{-1}. This last result for **8** in EtOH does not fully agree with the results expected from the simple picture. Although the observed positive first derivative component agrees with the expected shift to the region between **D** and **E**, one would also expect a substantial second derivative component which we do not observe. A possible explanation for this observed deviation with EtOH as solvent could be the formation of a direct interaction complex between the solute molecule and EtOH. The ΔA spectra of both **4** and **8** in mixtures of 2-MeTHF and EtOH exhibit an isosbestic point in ΔA (data not shown), pointing toward the presence of two distinct species. This specific interaction could be due to the formation of hydrogen bonds between the solvent and the solute and would lead to additional factors not considered in the qualitative analysis. By contrast, no such phenomenon can be observed in mixtures of toluene and 2-MeTHF.

For a more quantitative assessment of the solvent's influence on the electronic structure of these molecules the differences between a liquid and a frozen solvent matrix need to be considered. Since we study absorption effects that occur on a fast time scale compared with nuclear movements, the changes in the solvent's relaxation properties upon freezing will not affect these observables. The polarity of the solvent on the other hand will, as demonstrated above, dramatically affect the electronic structure for this class of molecules. Although there is no universally agreed upon definition of the term "solvent polarity", it can be viewed in the broadest and most general sense as the sum of interaction forces between the solvent and solute molecules.[11] For a given solvent−solute combination and changing temperature, a competition exists among these forces and the thermal motions of the molecules. Upon freezing the solvent, thermal motions are reduced drastically, and this will lead to a pronounced increase of the solvent polarity, the exact degree of which depends on the particular combination

(41) Blanchard-Desce, M.; Wortmann, R.; Lebus, S.; Lehn, J.-M.; Krämer, P. *Chem. Phys. Lett.* **1995**, *243*, 526−532.

(42) The studied compounds contained the dicyano acceptor group (as compounds **2** and **3** in this study) along with a dimethylanilino or a julolidine donor group.

(43) This relative independence of the ground state dipole moment and polyene chain length has recently been confirmed in other sets of donor/acceptor polyenes. Blanchard-Desce, M.; Alain, V.; Midrier, L.; Wortmann, R.; Lebus, S.; Glania, C.; Krämer, P.; Fort, A.; Muller, J.; Barzoukas, M. *J. Photochem. Photobiol. A* In press.

(44) Dähne, S.; Leupold, D.; Nikolajewski, H.-E.; Radeglia, R. *Z. Naturforsch.* **1965**, *20b*, 1006−1007.

(45) Radeglia, R.; Dähne, S. *J. Mol. Struct.* **1970**, *5*, 399−411.

(46) Radeglia, R.; Engelhardt, G.; Lippmaa, E.; Pehk, T.; Nolte, K.-D.; Dähne, S. *Org. Magn. Reson.* **1972**, *4*, 571−576.

of solvent and solute.[47] These effects will be discussed in detail in a forthcoming publication.[48]

The differences between the results obtained by Baumann[40] for **2** and **3** in liquid solvents and the values reported in frozen solvents here can be reconciled by taking these differences in solvent polarity into account even at a qualitative level. Similar to our results, Baumann reports values of $\Delta\mu$ that are strongly solvent dependent and also change across the absorption band for each individual solvent. Contrary to our results, he reports large values of $\Delta\mu$ that increase with increasing solvent polarity and reach 10 and 20 D for **2** and **3**, respectively, in liquid dioxane. Both the increase of $\Delta\mu$ in higher polar solvents and its magnitude thus place the compounds between limits **A** and **B**. An increase of the solvent's polarity, however, should move their position closer to the cyanine limit **C**, which is exactly the result obtained from the Stark spectra taken in frozen 2-MeTHF (*cf.* Figure 3).

A number of theoretical studies have investigated this solvent effect by modeling the solvent matrix with external electric charges that influence the ground state structure of a polyene bridge that is weakly perturbed by donor and acceptor end groups (e.g., compound **1**).[9,28,39] This approach allows for the integration of the solvent's influence on the polyene bridge with that of the end groups (i.e., donor/acceptor). For a weakly perturbed polyene like compound **1** it has been suggested that solvent effects should be relatively small, and this result has been generalized to all donor/acceptor polyenes.[28] The results presented here, however, demonstrate that the solvent effect can be quite large for a donor/acceptor polyene with stronger perturbation of the polyene bridge. The dramatic changes of the Stark spectra of compounds **4** and **8** upon changing the solvent's polarity (*cf.* Figure 7) clearly establish a pronounced dependence of the electronic structure of these molecules on the nature of the solvent environment. Compounds **4** and **8** are positioned in a region where the molecule's electronic structure is more sensitive to the influence of the solvent than compound **1**, and it would be interesting to see the results of calculations of solvent effects performed on molecules located in this region.

Absorption Spectra. Some of the results summarized above are mirrored in the compound's absorption spectra, i.e., its location, peak width, and the relative intensity of the vibronic side band. While the peak width reflects the amount of charge transfer upon excitation (i.e. $\Delta\mu$), the location of the absorption peak is expected to depend on the length of the conjugated chain and its amount of delocalization. For a cyanine-like structure (limit **C**), the absorption is expected to be at the lowest energy, which agrees well with our assignment of the solvent-dependent structures of **4** and **8**. Also, the absorption maximum of **4** is at lower energy than would be expected from its position within the series **4**−**8** due to the presence of an additional fused benzene ring in the acceptor group. The relative intensity of the vibronic side band also reflects the molecule's position within the limits **A**−**E**, being smallest at the cyanine limit. This can be understood by considering that a large amount of charge transfer will result in a large displacement of the excited state potential surface along the solvent reorganization coordinate leading to a larger degree of direct absorption into higher vibronic levels in the excited state.

Transition Polarizabilities. All compounds, except for **10**, show a negative zeroth derivative component in the region of the ΔA spectrum corresponding to the main absorption peak. The second parameter set, used to model the vibronic side band, shows a positive zeroth derivative component for all compounds, with the exception of **1** and **12**. As already mentioned, the contributions from the transition polarizability $\underline{A}$ and the transition hyperpolarizability $\underline{\underline{B}}$ to this term cannot be separated based on the experimental results. From eq 2 it can be seen that contributions from A are expected to be positive, while B can have both positive and negative contributions depending on the sign of its dominant tensor components. Since the measured ΔA spectra yield negative zeroth derivative components for the main absorption peak one can conclude that the dominant contribution derives from $\underline{\underline{B}}$. This assignment can also be justified on a theoretical basis, since for a strongly-allowed transition one can for parity reasons expect $\underline{A}$ to be rather small compared with $\underline{\underline{B}}$.[49] While this does not prove that the cross terms $A_{ij}\cdot\Delta\mu_j$ make a negligible contribution to the first derivative components of the ΔA spectra (eq 3), it does provide some justification for this assumption.

Electrooptic Heterogeneity. Differences in the electrooptic response of different vibronic bands were observed by Baumann in his study of **2**, **3**, and analogs in liquid solutions.[40] This was linked to changes of the transition moment, i.e., to different values of the transition polarizabilities, for different vibronic levels. He also speculated that there might be increasing values of $\Delta\mu$ with increasing transition energy across the absorption band, but could not clearly establish this based on the experimental data. Our analysis of the ΔA spectra demonstrates that a different set of electrooptic parameters is required to get good overall agreement of fit and data for the vibronic bands resolved in the absorption spectrum. The values of $|\Delta\mu|$ are consistently higher for the vibronic side band in all studied compounds (with the exception of **2**) and there are clear differences between the contributions of A and B to the ΔA signal of the main absorption and those to the vibronic side band.

Wortmann *et al.*[20] showed that for 1,8-diphenyl-1,3,5,7-octatetraene different vibronic levels are expected to show different electrooptic behavior. Experimentally determined parameters thus will reflect an average value of the simultaneously probed levels. They could model the molecule's electrooptic response by including vibronic mixing of the 1^1B_u and 2^1A_g states[50] via C−C stretching modes. Krawczyk and Daniluk[51] in a Stark spectroscopic study of carotenoids also observed deviations between data and fit in a region 1150 cm^{-1} toward higher energy from the main absorption peak. Since the energy gap between the 1^1B_u and 2^1A_g states is quite large in these compounds they argued that vibronic mixing of the

(47) Since for the compounds studied here the location of the absorption maximum is highly solvent dependent, it can be used to determine the polarity of the frozen solvent matrix. Based on such a comparison we can conclude that for **4**, **6**, **7**, and **8** the polarity of a frozen 2-MeTHF matrix corresponds to a polarity of liquid DMF to DMSO at room temperature. See: Bublitz, G. U.; Ortiz, R.; Runser, C.; Fort, A.; Barzoukas, M.; Marder, S. R.; Boxer, S. G. *J. Am. Chem. Soc.* **1997**, *119*, 2311−2312.

(48) Bublitz, G. U.; Boxer, S. G. In preparation.

(49) This can easily be seen from expressions for $\underline{A}$ and $\underline{\underline{B}}$ derived using perturbation theory: For the transition between the ground state (S_0) and first excited state (S_1) $A \propto \sum_i e^2\langle S_1|\mathbf{r}|i\rangle\langle i|\mathbf{r}|S_0\rangle$ and $B \propto \sum_i\sum_j e^3\langle S_1|\mathbf{r}|j\rangle\cdot\langle j|\mathbf{r}|i\rangle\langle i|\mathbf{r}|S_0\rangle$. The expression for $\underline{A}$ involves the interaction of both the ground state S_0 and the excited state S_1 with one virtual state i. For a strongly allowed transition S_1 will be of *ungerade* symmetry. Since S_0 is of *gerade* symmetry, the term for $\underline{A}$ will be symmetry forbidden. The expression for $\underline{\underline{B}}$ on the other hand involves two virtual states i and j. For i having *ungerade* symmetry and j *gerade* symmetry this term will be symmetry allowed.

(50) The electronic structure of polyenes exhibits the interesting feature of two close lying excited states, one of which is of ^1B_u symmetry and gives rise to an intense absorption feature, while transition to the other one is formally forbidden due to its ^1A_g symmetry. Although in donor/acceptor substituted polyenes it is not strictly true to speak of states with ^1A_g and ^1B_u symmetry, we will still use these terms for the two lowest excited states in order to label their main parentage.

(51) Krawczyk, S.; Daniluk, A. *Chem. Phys. Lett.* **1995**, *236*, 431−437.

1^1B_u state with higher states of the same symmetry was responsible for the observed deviations. They also noted that the observed large positive values of $\Delta\alpha$ provide a further indication for strong coupling between those states.

Our observation that the two sets of electrooptic parameters for all compounds exhibit common differences may reflect the properties of another excited state that vibronically couples into the main absorbing state. For donor/acceptor substituted polyenes the energy gap between the two lowest excited states decreases with increasing perturbation of the polyene bridge and vibronic coupling of the two states increases.[52] Thus in this set of compounds the differences of the electrooptic parameters should be due to mixing of the 2^1A_g state into the 1^1B_u state, and based on the common trend of an increased value of $|\Delta\mu|$ along with a decrease of $\Delta\alpha$, we expect the 2^1A_g state to have a large value of $|\Delta\mu|$ and small $\Delta\alpha$. This would also explain the positive values found for the zeroth derivative components of the vibronic side bands since an increased contribution from ^1A_g will lead to an increased magnitude of $\underline{A}$[49] and thus to a more positive zeroth derivative component. Interestingly, the side band's zeroth derivative term is the largest for the strongly perturbed polyenes **4**−**8** while for **1**, where the structure is more polyene-like, it is negative and the difference in $|\Delta\mu|$ between the two parameter sets is quite small. In this latter case the other mechanism of mixing with higher ^1B_u states might have significant contributions.

Limitations of the Physical Model. While the picture of a polyene bridge influenced by an electrostatic field has proven to be a powerful model for the explanation and integration of the effects of both donor and acceptor groups as well as those of changing the solvent, there are limits to its capabilities. One limitation is the description of the bridge by essentially one parameter (BLA or BOA), representing its degree of delocalization. Crystallographic data show that the bond lengths for all C−C bonds in the bridge can be different from each other. For example, for **1** the difference in length between adjacent C−C bonds increases, going from the donor to the acceptor end of the molecule.[8] Thus, while in our picture it is possible to have different donor/acceptor combinations such as weak/strong, strong/weak, and medium/medium each leading to the same amount of delocalization, they could, in fact, produce different bridge structures which might be reflected in the molecular electronic parameters.

The main trends of the expected evolution of the experimentally studied parameters $\Delta\alpha$ and $\Delta\mu$ with changing molecular structure (*cf*. Figure 8) were confirmed: a large value of $\Delta\mu$ at intermediate values of BLA/BOA and small $\Delta\mu$ and negative $\Delta\alpha$ around the cyanine limit **C**. The experimentally determined values of $\Delta\alpha$, as predicted, decrease with increasing delocalization of the polyene bridge up to the cyanine limit **C** and then increase again as the double bonds in the bridge again become more localized in region **D**. While the trends in the predicted and observed values of $\Delta\alpha$ agree with each other, the relative magnitudes disagree. The observed values of $\Delta\alpha$ are more positive than the predicted ones, i.e. very large for mostly localized bridge structures and less negative than predicted around limit **C**. The calculations, on the other hand, predict $\Delta\alpha$ to be of about equal magnitude but of different sign in limits **A** and **C**. This deviation could be due to an underestimate of the ground state polarizability α_g or an overestimate of the excited state polarizability α_e in the calculations. Assuming the general trends in the evolution of these corrected values of α_g or α_e vs BOA to be unchanged, this would lead to a curve of $\Delta\alpha$ vs BOA which would show better agreement with the observed $\Delta\alpha$ values. The observed basic trends—a decrease in $\Delta\alpha$ up to the cyanine limit **C** followed by an increase—would be conserved but the whole $\Delta\alpha$ vs BOA curve would be shifted toward more positive values of $\Delta\alpha$.[53]

Limitations of the Method. Deviations between data and fit were found in two different regions of the spectra. First, the small positive feature, which was observed on the low energy side of the ΔA spectrum of **1** (and to a lesser extent **5**, **6**, and **7**) and could not be accounted for in the fit, could be due to the small number of Gaussians that were used to fit the absorption data. The fact that the residuals of the absorption fits for these compounds are largest in this region at the red edge of the absorption band and the similar line shapes of the Stark and second derivative spectra in this region corroborate the view that this deviation is due to limitations of the fitting procedure.

Second, for nearly all the studied compounds there exists a deviation between the fit and the ΔA data from the main negative band of the ΔA spectrum on toward higher energy (*cf*. Figure 2). In the absorption spectra this corresponds to the region between the main absorption peak and the peak of the vibronic side band. This deviation could in part be due to the procedure of fixing the electrooptic parameters for the main band while fitting those for the side band. However, we do not believe that this explanation can fully account for those cases where the differences between data and fit are rather large and where they might arise from two different origins. One of these is the possibility of further vibronic heterogeneity of the absorption spectrum and its electrooptic parameters or the presence of an additional transition which is concealed by the main absorption peak.[54] On the other hand, for transitions with large values of $\Delta\alpha$ the contribution to $\Delta\mu$ induced by the surrounding solvent matrix is expected to change across the inhomogeneously broadened absorption band, leading to a variation of the overall $\Delta\mu$ across the absorption band.[55,56] The inclusion of this variability in $\Delta\mu$ in the fitting routine would require additional

(52) Kohler, B. E.; Spangler, C. W.; Westerfield, C. *J. Chem. Phys.* **1991**, *94*, 908−917.

(53) The differences between calculation and data might in part be due to the contribution of $A_{ij}\cdot\Delta\mu_j$ cross terms to the first derivative components of the ΔA spectra (eq 3) which were interpreted as being solely due to $\Delta\alpha$. However, assuming a derivative relationship (*cf*. ref 7) between the main components of the transition hyperpolarizability $\underline{A}$ and transition moment m, $A \propto dm/dF$, and using the calculated evolution of m vs BOA (not shown) and $\Delta\mu$ vs BOA (*cf*. Figure 8) of ref 9 this cross term is expected to be close to zero around the cyanine limit **C**. For an increasing polyene-like character of the bridge (i.e. upon going from **C** toward limit **A** or **E**) the relative contribution of the cross terms is predicted to increase. Accordingly, the reported values of $\Delta\alpha$ might be too large for those molecules assigned close to regions **B** or **D** if the absolute magnitude of this contribution turns out to be not negligible. However, since the trends in this calculated evolution of the cross-term contribution vs BOA and of $\Delta\alpha$ vs BOA are similar (decreasing from **A** to **C**, then increasing again), none of the assignments of the compounds (*cf*. Figure 8) would be affected.

(54) Further analysis of the residual to extract information on $\Delta\mu$ and $\Delta\alpha$ for this additional transition requires knowledge of the intensity and line shape of the transition's absorption band. For **10**, where the main absorption peak is quite narrow in comparison to the other compounds, an additional shoulder was observed in the region between the peaks of the main absorption and the vibronic side band. A global fit of the data including three sets of electrooptic parameters yielded the following parameters: $|\Delta\mu| = 1.7$ D and $\Delta\alpha = -10$ Å^3 for the main absorption peak, 0 D and 110 Å^3 for the shoulder, and 3.4 D and 90 Å^3 for the vibronic side band with zeroth derivative components of -1.8×10^{-3}, 0.08×10^{-3}, and 0.8×10^{-3}, respectively. The overall agreement between best fit and data is now quite good. Although it might be purely coincidental it is interesting to note that the parameters for this new band are very similar to the one result our model could not account for, namely **8** in EtOH. This shoulder could be either an additional vibronic level, a different electronic transition (e.g., for this strongly disturbed polyene system allowed $1^1A_g \rightarrow 2^1A_g$ absorption), or it could be due to a direct interaction of the donor and acceptor end groups since the connecting bridge is extremely short in this case.

(55) Vauthey, E.; Holliday, K.; Wei, C.; Renn, A.; Wild, U. P. *Chem. Phys.* **1993**, *171*, 253−263.

(56) Vauthey, E.; Voss, J.; de Caro, C.; Renn, A.; Wild, U. P. *Chem. Phys.* **1994**, *184*, 347−356.

independent fitting variables. We chose not do this since our goal was to explore the general trends of the electronic structure in donor/acceptor polyenes and thus to avoid additional complications in the fitting procedure which might introduce artifacts. The values of $|\Delta\mu|$ reported in Table 1 thus reflect an average value of a compound's difference dipole moment for a given absorption band, probably corresponding most closely to the value around the maxima of the absorption and vibronic peaks. The changes in $|\Delta\mu|$ across the inhomogeneously broadened band due to this effect are expected to be relatively small.[57]

Conclusions. For the 12 studied compounds the experimentally determined assignments to a location between limits **A** and **E** and trends in the values of $\Delta\mu$ and $\Delta\alpha$ agree well with those expected from the relative electron donating and accepting capabilities of the respective end groups. A moderately strong donor in combination with a weak acceptor group (compound **1**) leads to a slightly perturbed polyenic bridge structure (between limits **A** and **B**). A stronger acceptor end group shifts the molecule's location closer to limit **C** (compounds **2** and **3**). A similar result is found for compounds **4**−**8**: Compound **4** has a slightly weaker donor but much stronger acceptor end group than **1** and accordingly is located close to limit **B**. Again, with an increase of the acceptor strength (**5**−**8**) the ground state structure shifts toward a more charge separated form and for **8** the bridge structure is mostly delocalized (close to limit **C**). Further increase of the donor strength (compounds **11** and **12**) leads to a shift past limit **C**, and the bridge structure becomes more localized again.

A change in the polarity of the solvent matrix has a pronounced effect on the electronic structure (and thus on the position between limits **A** and **E**) of this class of molecules. Again, the observed changes and trends are consistent with expected ones, namely, a shift toward less polar ground state structures (closer to limit **A**) in nonpolar solvents and toward more polar ground state structures (closer to limit **E**) in polar solvents. Compound **4**, assigned to a position close to limit **B** in frozen 2-MeTHF, is shifted to a position between limits **A** and **B** in the less polar toluene and close to limit **C** in the highly polar EtOH. Compound **8**, due to its stronger acceptor end group already close to limit **C** in frozen 2-MeTHF, is shifted to a position between limits **B** and **C** in toluene and toward limit **E** in EtOH.

The influence of the donor, acceptor, and solvent on the electronic structure of donor/acceptor polyenes can effectively be described as an electric field effect. The end groups can be viewed as partial negative/positive charges placed at opposite ends of the polyene bridge. An increase in electron donor/acceptor strength of these substituents then would be equivalent to an increase in the negative/positive charge. Overall, this will lead to a polarization of the polyene bridge in its ground state. Depending on its polarity, the solvent will preferentially stabilize a more or less polarized ground state structure. This can be viewed as the effect of external charges interacting with those used to model the donor/acceptor end groups. In a further step of simplification the effect of this interaction can be reduced to a modification of the charges representing the donor/acceptor end groups, thus fully integrating the two effects. The good overall agreement between theoretical predictions and experimental data gives credence to this approach of modeling both donor/acceptor and solvent effects on the polyene bridge by electric fields,[58] which has been widely used in model calculations.[5,7,9,12,29−32]

Acknowledgment. We thank Dr. Fabienne Meyers for providing us with the results of the model calculations. This work was supported in part by grants from the National Science Foundation Chemistry Division (S.G.B.). The work was performed in part by the Jet Propulsion Laboratory, California Institute of Technology, as part of its Center for Space Microelectronics Technology and was supported by the Ballistic Missile Defense Organization, Innovative Science and Technology Office, through a contract with the National Aeronautics and Space Administration (NASA). Support at the Beckman Institute from the National Science Foundation (Grant No. CHE-9408701) and the Air Force Office of Scientific Research (Grant No. F49620-95-1-0178) is gratefully acknowledged. R.O. thanks the James Irvine Foundation for a postdoctoral fellowship.

JA9640814

(57) Assuming a maximum deviation of 20% between data and fit in ΔA and attributing all of this change to this origin, $|\Delta\mu|$ will change by maximal $\pm$10% across the inhomogeneously broadened band.

(58) Differences, however, do exist between *internal* electric field effects (such as those produced by the end groups) and *external* ones (such as those of the solvent matrix) with regard to the heterogeneity of the electrooptic parameters. This was demonstrated in a Stark spectroscopic study of the carotenoid derivative spheroidene which is one of the chromophores of the B800-850 antenna complex protein. [Gottfried, D. S.; Steffen, M. A.; Boxer, S. G. *Biochim. Biophys. Acta* **1991**, *1059*, 76−90 and *Science* **1991**, *251*, 662−665]. Embedded in a nonpolar organic glass spheroidene shows only moderately small values of $|\Delta\mu| < 4.7$ D. However, for the same chromophore, now at its position inside the protein, this value changes dramatically and $|\Delta\mu| \approx 15$ D for the main absorption peak as well as for all vibronic side bands. This large $|\Delta\mu|$ is apparently due to the effect of the protein matrix on the electronic structure of the chromophore—effectively an *external* field effect. A comparably large value of $|\Delta\mu| \approx 20$ D was found for the main absorption peak of spheroidenone (an acceptor substituted derivative of spheroidene) embedded in a nonpolar organic glass—an *internal* field effect. However, in this case the vibronic side bands clearly show some variation in their $|\Delta\mu|$ values. Even larger differences in the electrooptic response of different vibronic bands have been found for other acceptor substituted carotenoids where the acceptor group is very strong [Bublitz, G. U.; Boxer, S. G. Unpublished results].